



This is a repository copy of *The second messenger c-di-AMP inhibits the osmolyte uptake system OpuC in Staphylococcus aureus.*

White Rose Research Online URL for this paper:
<http://eprints.whiterose.ac.uk/104059/>

Version: Accepted Version

Article:

Schuster, C.F., Bellows, L.E., Tosi, T. et al. (4 more authors) (2016) The second messenger c-di-AMP inhibits the osmolyte uptake system OpuC in *Staphylococcus aureus*. *Science Signaling*, 9 (441). ra81-ra81. ISSN 1945-0877

<https://doi.org/10.1126/scisignal.aaf7279>

Reuse

Items deposited in White Rose Research Online are protected by copyright, with all rights reserved unless indicated otherwise. They may be downloaded and/or printed for private study, or other acts as permitted by national copyright laws. The publisher or other rights holders may allow further reproduction and re-use of the full text version. This is indicated by the licence information on the White Rose Research Online record for the item.

Takedown

If you consider content in White Rose Research Online to be in breach of UK law, please notify us by emailing eprints@whiterose.ac.uk including the URL of the record and the reason for the withdrawal request.



eprints@whiterose.ac.uk
<https://eprints.whiterose.ac.uk/>

The second messenger c-di-AMP inhibits the osmolyte uptake system OpuC in *Staphylococcus aureus*

Christopher F. Schuster^{1&}, Lauren E. Bellows^{1&}, Tommaso Tosi¹, Ivan Campeotto^{1,3}, Rebecca M. Corrigan^{1,2}, Paul Freemont⁴, Angelika Gründling^{1*}

¹Section of Microbiology and MRC Centre for Molecular Bacteriology and Infection, Imperial College London, London SW7 2AZ, UK; ²Present address: Department of Molecular Biology and Biotechnology, University of Sheffield, Sheffield, S10 2TN, UK,

³Present address: Department of Biochemistry, University of Oxford, Oxford OX1 3QU

⁴Section of Structural Biology, Department of Medicine, Imperial College London, London SW7 2AZ, UK

*Address correspondence to Angelika Gründling, a.grundling@imperial.ac.uk

& equal contributions

ABSTRACT

Staphylococcus aureus is an important opportunistic human pathogen that is highly resistant to osmotic stresses. In order to survive an increase in osmolarity, bacteria immediately take up potassium and small organic compounds, also referred to as compatible solutes. The second messenger c-di-AMP binds to several receptor proteins, most of which are involved in ion and potassium uptake, that help bacteria cope with osmotic stress. In this study, we identified OpuCA, the ATPase component of an uptake system for the compatible solute carnitine, as a c-di-AMP target protein in *S. aureus* and found that a strain overproducing c-di-AMP showed reduced carnitine uptake. The CBS domains of OpuCA bound to c-di-AMP, and a crystal structure revealed a putative binding pocket for c-di-AMP in the cleft between the two CBS domains. Thus, c-di-AMP is involved in regulating both branches of osmoprotection (potassium uptake and compatible solute uptake), suggesting that c-di-AMP is a general osmotic stress regulator.

INTRODUCTION

Signaling nucleotides are key molecules utilized by bacteria to coordinate different cellular processes in order to rapidly respond to environmental changes. Cyclic diadenosine monophosphate (c-di-AMP) is one such signaling nucleotide produced predominantly by Gram-positive bacteria (1, 2). This di-nucleotide is produced from two molecules of adenosine triphosphate (ATP) by diadenylate cyclase enzymes containing an N-terminal DisA domain and degraded to 5'-phosphoadenylyl (3'→5')-adenine (pApA) or adenosine monophosphate (AMP) by phosphodiesterase enzymes containing either DHH-DHHA1 domains or a His-Asp (HD) domain (3-5). In *Staphylococcus aureus*, c-di-AMP is produced by the adenylylate cyclase DacA

and degraded by the phosphodiesterase GdpP and intracellular c-di-AMP concentrations of 2 to 8 μM have been determined (6-8). For optimal bacterial growth, fine control of intracellular c-di-AMP concentration is critical because both high and low concentrations negatively impact proliferation (7, 9, 10). Indeed, in various Gram-positive bacteria, it has been shown that c-di-AMP production is essential for growth in rich medium (7, 10, 11). In *Listeria monocytogenes* it has been reported that the absence of c-di-AMP leads to a metabolic imbalance and a toxic accumulation of the stringent response alarmone (p)ppGpp, which causes growth arrest (12). However, the exact molecular details leading to the metabolic imbalance have not yet been established, and it is also not known if a similar mechanism exists in other bacteria.

c-di-AMP functions as signaling molecule by binding to and regulating the activity of specific receptor proteins. One essential receptor is the central carbon metabolism enzyme pyruvate carboxylase (PC) of *L. monocytogenes* (13). Other c-di-AMP target proteins identified in *L. monocytogenes* include NrdR, a transcription repressor controlling the expression of deoxyribonucleotide biosynthesis genes as well as CbpA and CbpB, cystathionine beta synthase (CBS) domain pair proteins of unknown function (13). While this work was in revision, OpuCA, the ATPase component of the osmolyte uptake system OpuC, and yet another CBS domain protein, was identified as additional c-di-AMP receptor in *L. monocytogenes* (14). The first protein found to bind c-di-AMP was the *Mycobacterium smegmatis* protein DarR, a transcription factor that controls the expression of genes involved in fatty acid biosynthesis (15). Another class of c-di-AMP target protein is the P_{II}-like signal transduction protein known as PstA in *L. monocytogenes* and *S. aureus* or DarA in *Bacillus subtilis* (13, 16, 17). Whereas several apo- and nucleotide-bound structures have been solved for these proteins, their cellular functions are still unknown (17-20).

The remaining known c-di-AMP target proteins are part of ion transport systems or are involved in the regulation of ion transport (16). Specifically, these include the *S. aureus* sensor histidine kinase KdpD, which is required to activate the expression of genes encoding components of the ATPase-type potassium uptake system Kdp (16). c-di-AMP binds to the universal stress protein (USP) domain in KdpD, and this may inhibit KdpD function (21). Other target proteins are the *B. subtilis* and *S. aureus* KtrA proteins (also referred to as KtrC in *S. aureus*) and a homologous protein in *S. pneumoniae* called CabP (16, 22). These proteins are the cytoplasmic gating components of a second type of potassium transport system (16, 22). c-di-AMP binding to these potassium transporter gating components is also thought to inhibit potassium uptake (16, 22). c-di-AMP interacts with the C-terminal RCK_C domain in KtrA (16, 23). This domain is also present in the *S. aureus* monovalent cation-proton antiporter CpaA, which may catalyze the efflux of Na⁺ or K⁺ from the cytoplasm in exchange for extracellular H⁺ (16, 24, 25). In this case, c-di-AMP binding has been reported to increase the activity of the antiporter (24). Altogether these findings suggest that c-di-AMP inhibits potassium uptake and reduces cellular potassium concentrations.

Potassium uptake systems and cation-proton antiporters together with transporters of specific amino acids and small organic molecules (compatible solutes) are key components helping bacteria to cope with environmental pH fluctuations and high salt or osmolality conditions. As an immediate response to an increase in the extracellular salt concentration, bacteria take up potassium to counteract the toxic accumulation of Na⁺ in the cell and to prevent the efflux of water (26, 27). In addition to potassium uptake, bacteria also acquire or synthesize compatible solutes such as glycine-betaine, choline, carnitine and proline (27, 28).

In this work, we identified OpuCA, a component of the cytoplasmic ATPase that functions in the *S. aureus* ATP-binding cassette transport system OpuC, as new c-di-AMP receptor protein. We show that c-di-AMP interacts specifically and with physiologically relevant strength with the C-terminal CBS domain of OpuCA. We further show that the *S. aureus* OpuC system is a functional carnitine uptake system and present evidence that high intracellular concentrations of c-di-AMP inhibit carnitine uptake. With this we provide experimental evidence that both arms of osmoprotection – the potassium and osmolyte uptake systems – are part of the c-di-AMP regulatory network.

RESULTS

Binding of c-di-AMP to the CBS domain of *S. aureus* OpuCA

In previous work, we identified three c-di-AMP target proteins, (KtrA, KdpD and PstA) using the differential radial capillary action of ligand assay (DRaCALA) with an *S. aureus* ORFeome library that enables the production of 2,335 N-terminally His-tagged proteins from *S. aureus* strain COL in *E. coli* (16). Here, we screened an *S. aureus* COL ORFeome library of 2,337 histidine and maltose binding protein (His-MBP)-tagged fusion proteins (29) in an attempt to identify additional c-di-AMP-interacting proteins. The DRaCALA screen was performed in 96-well format (16, 29, 30) and, as expected, positive interactions were detected for the His-MBP-KtrA, His-MBP-KdpD and His-MBP-PstA fusion proteins. In addition, we detected an interaction between c-di-AMP and the His-MBP-SACOL2453 fusion protein (Fig. S1). SACOL-2453 corresponds to protein SAUSA300_2393 in *S. aureus* strain FPR3757 and is annotated as OpuCA. *opuCA* is one of four genes in the *opuCA-opuCD* operon (Fig. 1A), which encodes the ATP-binding cassette osmoprotectant uptake system OpuC. The OpuC system is composed of

the transmembrane components OpuCB and OpuCD, a predicted lipoprotein OpuCC, serving as substrate binding protein, and OpuCA, constituting the cytoplasmic ATPase component (Fig. 1B). To confirm that OpuCA is indeed a *bona fide* c-di-AMP target protein, we isolated the plasmid from the *E. coli* library strain and confirmed that its sequence corresponded to *opuCA* before introducing the plasmid into a *E. coli* strain T7IQ. We induced production of the His-MBP-OpuCA fusion protein and purified it by Ni-NTA affinity and size exclusion chromatography. The purified protein solutions ranged in concentration from 50 μM to 0.1 μM and were diluted two-fold for use in DRaCALAs. DRaCALAs revealed a K_d of $2.46 \pm 0.14 \mu\text{M}$ for the interaction of c-di-AMP with the purified His-MBP-OpuCA fusion protein (Fig. 1C). This interaction was specific to c-di-AMP, because only an excess of unlabelled c-di-AMP, but not an excess of other nucleotides, could compete with radiolabeled c-di-AMP for binding to His-MBP-OpuCA (Fig. 1D). Taken together, these data indicate that the *S. aureus* OpuCA protein is a c-di-AMP-binding protein that interacts specifically and with physiological strength with this signaling nucleotide.

The ATPase domain of OpuCA spans amino acids 38-194, and the two cystathione beta synthase (CBS) modules are at amino acids 251 to 302 (CBS1) and 314 to 363 (CBS2) (Fig. 2A). CBS domains are usually found in pairs, and hereafter we collectively refer to this pair as the CBS domains. To determine which domain of OpuCA interacts with c-di-AMP, we generated constructs for expressing and purifying the ATPase and CBS domains separately. We purified the His-MBP, His-MBP-OpuCA, His-MBP-ATPase (OpuCA residues 1 to 262), and His-CBS (OpuCA residues 237 to 408) fusion proteins alongside the His-MBP and His-MBP-OpuCA control proteins (Fig. 2B). These purified proteins were subsequently used in DRaCALAs with radiolabeled c-di-AMP. This analysis revealed that c-di-AMP interacted with the CBS domain of

OpuCA but not the ATPase domain (Fig. 2C). His-CBS interacted with c-di-AMP with a K_d of $2.86 \pm 0.14 \mu\text{M}$ (Fig. 2D). This interaction was specific because only an excess of unlabelled c-di-AMP, but not any of the other nucleotides tested, could compete for binding (Fig. 2E).

c-di-AMP interaction with other *S. aureus* CBS domain-containing proteins

Two *L. monocytogenes* proteins of unknown function that each consist of a stand-alone CBS domain, CbpA (Lmo0553 in strain EGD-e) and CbpB (Lmo1009 in strain EGD-e), have been identified as c-di-AMP receptors (13). No stand-alone CBS domain protein is predicted to be encoded in the *S. aureus* COL genome. However, besides OpuCA, the conserved domain database (CDD) contains six other *S. aureus* COL proteins that contain CBS domains in addition to other domains. Specifically, these proteins are predicted to encode the inosine-5' monophosphate dehydrogenase GuaB (SACOL0460), two membrane proteins with unknown functions (SACOL0762 and SACOL0921), the magnesium transporter MgtE (SACOL1013), the transcription factor CcpN (SACOL1621), and a multi-domain cytoplasmic protein of unknown function (SACOL1752). Sequence alignments comparing the CBS domains of OpuCA with the CBS domains of these other *S. aureus* proteins (including 10 the amino acids flanking each end of the CBS domains) revealed that these domains share only 10–23 % sequence identity (Fig. 3A). *E. coli* strains producing a His-MBP fusion to four of these proteins [SACOL0460 (GuaB), SACOL0921, SACOL1013 (MgtE), and SACOL1621 (CcpN)] were present in the *S. aureus* ORFeome library, however none of these fusion proteins interacted with c-di-AMP in the initial screen. To confirm the absence of interaction with c-di-AMP, we verified the sequence of the inserts of these clones. In addition, we constructed plasmids pVL847-SACOL0762, pVL847-SACOL0921, and pVL847-SACOL1013 to overexpress only the CBS domains of these

transmembrane proteins in *E. coli* in order to reduce the likelihood of misfolding and increase protein production. We also constructed plasmid pVL847-SACOL1752 because this protein was not present in the ORFeome library used for the initial screen. Subsequently, we optimized the growth conditions so that protein bands could be detected on a Coomassie stained gel for all His-MBP fusion proteins (Fig. 3B). Next, we performed DRaCALAs with these *E. coli* lysates and found that OpuCA, but none of the other *S. aureus* proteins containing CBS domains, bound to c-di-AMP (Fig. 3C). To exclude the possibility that some proteins were present in inclusion bodies and therefore inaccessible for binding to c-di-AMP, lysates were cleared of insoluble inclusion bodies by centrifugation (Fig. S2A) and DRaCALAs repeated using lysates lacking insoluble proteins. None of the cleared lysates, including those from cells expressing OpuCA, exhibited detectable binding to c-di-AMP (Fig. S2B). However, the observation that whole lysates from cells expressing OpuCA bound to c-di-AMP indicates that proteins are still able to interact with c-di-AMP even if they are present in insoluble aggregates. Taken together, these data show that c-di-AMP interacts specifically with the paired CBS domain of OpuCA, but does not interact with other *S. aureus* proteins that contain CBS domains under the same experimental conditions.

Crystal structure of the *S. aureus* OpuCA CBS domain

To gain insight into the structure of the c-di-AMP-binding CBS domain in *S. aureus* OpuCA, we purified and crystallized the His-CBS fusion protein, which contains OpuCA residues 237 to 408 (Fig. 4A, 4B and Table S1). The CBS1 (residues 250-306) and CBS2 (residues 320-369) modules have a highly similar $\beta\alpha\beta\alpha$ fold and can be superimposed with a total rmsd of 0.75 Å (Fig. 4A). The CBS1 and CBS2 domains are connected by a linker region to form a so-called

“Bateman” fold, as seen in other paired CBS domain pair structures (31). The N- and C-terminal portions of His-CBS (residues 237-249 and 370-408 of OpuCA, respectively) were not observed in the electron density map, suggesting that these regions are disordered. The crystal structure was solved as a tetramer in the asymmetric unit, but further inspection showed that the asymmetric unit was composed of two distinct protein dimers (Fig. S3A). An analysis with the PdbEPIA server (32) revealed that a large surface area of $\sim 800 \text{ \AA}^2$ was buried at the monomer-monomer interface, suggesting that dimerization might be physiologically relevant rather than merely a result of crystallization. Indeed, a size-exclusion chromatography–multi-angle light scattering (SEC-MALS) analysis of the purified His-CBS protein, which is 21.8 kDa in size, indicated that the protein is dimeric in solution, because the migration of the protein corresponded to an ~ 36 kDa protein complex (Fig. S3B). To find structural homologues of the OpuCA CBS domain, we submitted the coordinates to the PdbFold server (33). The CBS domain protein MJ0100 from *Methanocaldococcus jannaschii* (PDB code 3KPB) was identified as the closest homologue with a Z-score of 8.6 and an rmsd of $\sim 1.7 \text{ \AA}$. We solved the structure of MJ0100 in complex with its ligand S-Adenosyl-Methionine (SAM), which bound in a cleft between CBS1 and CBS2 (Fig. 4C) (34). Several other “Bateman” module structures in either an apo or ligand-bound form are available (35). In most cases, the ligand is AMP, ADP, ATP or SAM, and the nucleotide is bound at a site equivalent to the SAM-binding site in MJ0100. The adenine base of SAM in MJ0100 was stabilized by hydrophobic residues, whereas the ribose moiety made polar contacts with D439 (34) (Fig. 4C). An electrostatic potential calculation of the MJ0100 SAM-binding site using APBS (36) showed that the binding site has a positively charged electrostatic surface (Fig. 4D). A structural overlay of the OpuCA CBS domain with the MJ0100 protein, followed by APBS analysis, showed that the OpuCA CBS domain also has a

positively charged cleft at the location corresponding to the SAM binding site in protein MJ0100 (Fig. 4D). This suggests that the binding site for the c-di-AMP ligand might be at a similar location. A structure-based sequence alignment of ten CBS domain structures solved in a nucleotide ligand-bound form (Fig. S4), revealed that in all cases the ligand was bound in a cleft between the $\beta 2$ - $\alpha 2$ region of CBS1 and the $\alpha 1$ - $\beta 1$ - $\beta 2$ region of CBS2. However, no unique nucleotide binding amino acid motif could be identified. Taken together, our data show that the *S. aureus* OpuCA CBS has a typical “Bateman” fold and, based on analogy with other nucleotide-binding CBS domains, we speculate that the c-di-AMP ligand might bind at a cleft between the CBS domain pair.

Identification of OpuCA variants unable to bind c-di-AMP

Next, we set out to identify amino acid residues in OpuCA that are important for c-di-AMP binding. In the absence of a structure of OpuCA in complex with c-di-AMP, we made use of information from previously solved structures of c-di-AMP binding proteins in complex with the nucleotide ligand (13, 17-20, 23, 24). In most cases aromatic amino acids including tyrosine (Tyr, Y) or phenylalanine (Phe, F) residues provided key base stacking interactions with the nucleotide ligand. To test if aromatic amino acids are also essential for the interaction of c-di-AMP with the CBS domain of OpuCA, residues Phe²⁸³, Phe²⁹⁴, Tyr³¹⁹, Tyr³⁶⁵ and Trp³⁶⁹ were individually mutated to alanines. In addition, two variants of the CBS domain with C-terminal deletions were made by truncating the protein at position 365 (CBS Δ 365) or 374 (CBS Δ 374). We produced the respective His-tagged CBS variants in *E. coli* and prepared lysates from these strains as well as from *E. coli* strains producing wild-type His-CBS or containing an empty pET28b vector as positive and negative controls, respectively. Although the exact amount of

overproduced protein His-tagged CBS protein variants cannot be quantified in crude extracts, aliquots of these lysates were analyzed by gel electrophoresis, to confirm qualitatively that similar amounts of protein were produced (Fig. 5A). Next, the lysates were diluted 1:10 and used in DRaCALAs to assess the ability of the different variants to interact with c-di-AMP (Fig. 5B). Three variants, specifically the His-CBS^{F283A} and His-CBS^{F294A} single amino acid substitution variants and the CBS Δ 365 variant, showed drastically reduced binding. Attempts to purify His-CBS Δ 365 failed, indicating that this protein does no longer fold properly, and hence this variant was not further characterized. On the other hand, His-CBS^{F283A} and His-CBS^{F294A} were readily purified by Ni-NTA and size exclusion chromatography. Next, we set out to determine the binding affinities between c-di-AMP and the purified variants. At the highest protein concentration some binding was observed for His-CBS^{F283A} and His-CBS^{F294A}, saturation was not reached, hence no actual K_d values could be determined for these variants binding to c-di-AMP (Fig. 5C). Taken together, this analysis suggests that Phe²⁸³ and Phe²⁹⁴ might interact with the c-di-AMP ligand. Next, the locations of the Phe²⁸³ and Phe²⁹⁴ residues were mapped onto the *S. aureus* OpuCA CBS crystal structure. Both residues are located within the cleft, which corresponds to the nucleotide-binding site in other CBS domain proteins solved in the presence of the ligand. This structural analysis combined with the mutagenesis study indicates that the aromatic amino acids Phe²⁸³ and Phe²⁹⁴ play a critical role in nucleotide binding. In addition, the location of these residues on the structure further supports the notion that c-di-AMP binds to OpuCA in a positively charged groove located at the interface between CBS1 and CBS2.

Physiological characterization of the *S. aureus* OpuC transporter

To assess the physiological function of the OpuC transporter in *S. aureus*, we conducted uptake assays. A previous study by Kiran *et al.*, suggested that the *S. aureus* OpuC system is a choline transporter (37). We therefore tested the uptake of radiolabeled choline as described in Kiran *et al.* (37) using the wild-type *S. aureus* strain LAC* (WT), LAC* cells lacking *opuCA* (Δ *opuCA*), and a complementation strain in which OpuCA was expressed from a plasmid in Δ *opuCA* cells (*opuCA* complementation). Radiolabeled choline accumulated over time in samples derived from the WT strain, showing that choline is taken up by *S. aureus* (Fig. 6A). However, the rate of choline uptake was identical for the WT, Δ *opuCA*, and *opuCA* complementation strains, suggesting that the OpuC system is not the main choline uptake system in *S. aureus* (Fig. 6A). To minimize the amount of available compatible solutes in the medium while also increasing the osmotic stress, we repeated the experiment in chemically defined medium (CDM) containing 0.5 M NaCl. Choline was taken up efficiently, but again there was no difference in the uptake rate between the WT, Δ *opuCA* mutant, and *opuCA* complementation strain (Fig. 6B). We confirmed by Western-blot the production of OpuCA protein in the WT strain grown under these conditions (Fig. S5). As expected, the protein was absent in the Δ *opuCA* strain and again present at slightly reduced amounts compared to WT in the *opuCA* complementation strain (Fig. S5). Next we tested if the OpuC system is involved in the uptake of the compatible solutes glycine betaine or carnitine, which have been shown to be substrates for the *B. subtilis* and *L. monocytogenes* OpuC systems, respectively (38, 39). As seen for choline, radiolabelled glycine betaine was taken up at a similar rate by the WT, Δ *opuCA*, and *opuCA* complementation strains, indicating that the OpuC system is not the main glycine betaine uptake system in *S. aureus* (Fig. 6C). In contrast, accumulation of radiolabelled carnitine was only observed in the WT and *opuCA* complementation strains but not in the Δ *opuCA* strain, indicating that the OpuC system is the

main carnitine uptake system in *S. aureus* (Fig. 6D). Finally, to test whether c-di-AMP plays a role in influencing the activity of the OpuC transporter, carnitine uptake was compared between the WT LAC* strain and strain LAC* Δ *gdpP*, which was previously reported to produce approximately 10-fold higher intracellular concentrations of c-di-AMP (2, 7). The accumulation of carnitine was measured over 4 hours. A significant reduction in the amount of retained radiolabeled carnitine was observed for the Δ *gdpP* strain at early time points (t = 1 h and 2 h) (Fig. 6E). The total amount of carnitine retained in the WT and Δ *gdpP* strains was similar at later time points, presumably reflecting the steady state. Taken together, these data suggest that c-di-AMP negatively impacts the activity of the *S. aureus* OpuC transporter.

DISCUSSION

Osmotic stress has a profound impact on the structure, chemistry, and physiology of a bacterial cell. Therefore, osmotic stress adaption and tolerance mechanisms are key for the survival and growth of bacteria in their natural environments (27). As a countermeasure to an osmotic upshift, bacteria take up potassium ions and osmolytes (27). The two main potassium transport systems in *S. aureus* are the Ktr- and Kdp-type transporters (40, 41). Components of both these systems have been identified as receptor proteins for the signaling nucleotide c-di-AMP (16). Here, we identified the *S. aureus* OpuCA protein, a cytoplasmic ATPase component of an osmolyte uptake system, as an additional c-di-AMP target protein (Figs. S1 and 1). With this, we implicate this signaling molecule as a potential regulator of both arms of osmoprotection in this organism.

Bacteria can accumulate many different types of osmolytes, including glycine betaine, choline, proline, trehalose, and carnitine (42). We found that the uptake of carnitine is abolished

in an *opuCA* mutant strain (Fig. 6D), suggesting that OpuC is the main or only functional carnitine uptake system in *S. aureus* under the conditions tested. In contrast to a previous report (37), choline accumulated in the wild-type and the *opuCA* deletion strain at nearly identical rates in our hands (Figs. 6A and 6B). Several different Opu transporters have been identified in *B. subtilis* and their substrate specificity and role in the osmotic stress tolerance characterized (43). The three main types are the multi-component ATP-binding cassette transport systems OpuA, OpuB, and OpuC, the homo-trimeric BCCT-type glycine betaine transporter OpuD, and the sodium:solute symporter family (SSF) proline transporter OpuE (28, 43). Much less is known about the various osmoprotectant uptake systems in *S. aureus*. Our bioinformatics analysis suggests that, in addition to OpuC, *S. aureus* encodes a second ATP-binding cassette transport system (Fig. S6). This system is most closely related to the *B. subtilis* OpuB system and will therefore be referred to as such. It is composed of the cytoplasmic ATPase component OpuBA and the membrane and periplasmic substrate-binding fusion protein OpuBB-BC (Fig. S6). Furthermore, *S. aureus* has three distinct BCCT-type transport systems, here referred to as OpuD1, OpuD2 and BccT (or CudT) (Fig. S6). Although these BCCT-type transporters are most closely related to systems that transport choline, glycine betaine, or both, it has been shown that OpuD1 is also a low-affinity proline uptake system (44). Lastly, a sodium-solute symporter family (SSF) transporter called PutP is present in *S. aureus* (Fig. S6). PutP is a high affinity proline uptake system and its expression is activated under high osmolarity conditions and during infection of murine and human tissues (45). Of these systems, we identified only the OpuC osmoprotectant uptake system as a target for c-di-AMP. Using a strain producing high concentrations of c-di-AMP, we present experimental evidence that suggests that this signaling nucleotide negatively impacts carnitine uptake (Fig. 6E). Additional work is required to better

define the roles of the different osmoprotectant uptake systems in *S. aureus* osmotic stress adaption, to determine whether OpuC is indeed the only osmoprotectant transporter that is part of the c-di-AMP signaling network, and to investigate the biological importance of c-di-AMP-mediated regulation of OpuC during osmotic stress adaption and infection.

c-di-AMP binds specifically to the C-terminal CBS domains of the *S. aureus* OpuCA protein (Fig. 2). The CBS domains in OpuAA of the *Lactococcus lactis* OpuA system have an important regulatory function and serve as a sensor of the intracellular ionic strength (46-48). Under low ionic strength conditions, positively charged surface-exposed residues in this domain are thought to interact with the anionic phospholipids in the membrane, resulting in low transport activity (48). High ionic strength is thought to interrupt this membrane interaction, leading to increased transport activity (48). However, these positively charged regulatory residues are absent in the *S. aureus* OpuCA protein, indicating that the regulatory mechanism is likely very different between these systems. Based on the results presented in this study, we suggest that c-di-AMP and perhaps even other nucleotides can post-transcriptionally regulate CBS-domain-containing ATP-binding cassette Opu transporters. It is unclear to what extent and how c-di-AMP modulates the activity of the *S. aureus* OpuC system. From a mechanistic point of view, it seems plausible that binding of c-di-AMP to the CBS domain would influence the ATPase activity of OpuCA and thereby regulate uptake rates. To address this question, further in vitro investigations are needed. When we overproduced and purified the full-length OpuCA protein, the protein had very weak ATPase activity, which was not sensitive to the concentration of c-di-AMP. Therefore, for further studies on the regulation of transporter activity it is likely that the full ABC transporter complex in a lipid environment will be required to reconstitute ATPase activity comparable to native hydrolysis rates.

CBS domains are not only present in bacterial proteins, they are important regulatory domains found in many functionally unrelated proteins across all domains of life (35, 49). Several hereditary human diseases have been linked to mutations in CBS domains, hence enzymes and transporters containing such domains have been the focus of numerous biochemical and structural studies (see reviews (35, 49)). From these studies it is known that CBS domains usually come in pairs (as observed in the *S. aureus* OpuCA protein), assume a “Bateman” fold, and can bind different nucleotide ligands, most often in a cleft formed between the CBS1 and CBS2 domains (see review (35)). The structure presented in this work revealed that the *S. aureus* OpuCA CBS1 and CBS2 domains assume the expected “Bateman” fold (Fig. 4 and S3). Although we were only to obtain the apo-structure at this point, we can still make inferences as to the location of the c-di-AMP binding site, based on mutagenesis experiments performed in this study and available structures of other CBS domains that have been determined in a ligand-bound state. A positively charged cleft is formed in OpuCA between the CBS1 and CBS2 domains (Fig. 4D), matching the SAM binding pocket of MJ0100 and the AMP-binding site in other CBS domain proteins (34, 35), indicating that c-di-AMP could bind here. Furthermore, changing two phenylalanine residues in this proposed binding pocket, Phe²⁸³ and Phe²⁹⁴, to Ala drastically decreased the binding affinity for c-di-AMP (Fig. 5). This is presumably due to abolishing a base stacking interaction between the side chain of these amino acids and the adenine base in c-di-AMP. Up to now three different CBS domain proteins have been identified as specific c-di-AMP target proteins; namely the *L. monocytogenes* standalone CBS domain proteins of unknown function CbpA and CbpB (13) and the *S. aureus* OpuCA protein. However, these three c-di-AMP binding CBS domain proteins share only limited similarity at the sequence level and have no readily identifiable, specific c-di-AMP binding motif. Therefore, it is currently

not possible to predict in silico which CBS-domain-containing proteins will interact specifically with c-di-AMP without performing binding experiments. While this manuscript was in revision, the OpuCA protein from *L. monocytogenes* was also identified as c-di-AMP receptor protein and the structure of its CBS domains in the c-di-AMP bound state reported (14). In the *L. monocytogenes* protein, one c-di-AMP nucleotide was bound per OpuCA dimer with the two adenine bases contacting the protein in a cleft between the CBS1 and CBS2 domains within each monomer (14). It will be interesting to investigate in future work whether the nucleotide binding sites are identical in both proteins, particularly because the dimer configuration appeared to be quite different for the two proteins (14). It is noteworthy that in *L. monocytogenes* a total of three CBS-domain proteins, the multi-domain protein OpuCA and the stand-alone CBS domain proteins CbpA and CbpB, have thus far been implicated as c-di-AMP receptor proteins (13, 14). In *S. aureus*, which lacks standalone CBS-domain proteins, OpuCA was the only CBS-domain protein to show binding to c-di-AMP in DRaCALAs (Fig. 3). Other *S. aureus* multi-domain CBS proteins did not bind c-di-AMP in DRaCALAs, suggesting that these other CBS-domain containing proteins likely are not c-di-AMP receptors.

For several bacterial species, it has now been shown that an increase in intracellular c-di-AMP concentrations leads to salt hypersensitivity (16, 50), but the molecular mechanism leading to this phenotype is not yet completely understood. The identification of components of potassium transport systems and now of an osmolyte uptake system as c-di-AMP receptors brings us a step closer, as inhibition of such transporters will lead to a decrease in osmotic stress tolerance. Increased intracellular c-di-AMP concentrations have also been associated with an increased resistance to heat, antibiotics, and low pH, processes in which potassium and osmolyte transporters also have important functions (4, 16, 50-54). Appropriate adjustments in cellular

potassium concentrations are key for pH homeostasis and maintenance of membrane potential, and osmolytes have been implicated not only in osmotic stress tolerance but also in resistance to heat or cold, because their accumulation helps to stabilize proteins under these stress conditions. Why in this case increased c-di-AMP concentrations and an interaction of c-di-AMP with potassium and osmolyte transporter components leads to increased heat or cold resistance warrants further investigation. But clearly the identification and characterization of additional c-di-AMP receptor proteins, as conducted in this study, is an important step towards elucidating the regulatory network of this widespread signaling molecule.

MATERIALS AND METHODS

Bacterial strains and growth conditions

Bacterial strains used in this study are listed in Table S2. *E. coli* strains were grown in Lysogeny Broth (LB) or LB-M9 (49.3 mM Na₂HPO₄, 14.7 mM KH₂PO₄, 8.55 mM NaCl, 18.7 mM NH₄Cl, 3.7 mM Na succinate, 11.1 mM glucose, 2 mM MgSO₄, 1% tryptone, 0.5% yeast) medium and *S. aureus* strains in Tryptic Soy Broth (TSB), Chemically Defined Medium (CDM) or M9 medium at 37°C with aeration (180 rpm). The M9 medium was prepared as described in (55) with 0.2% glucose as the carbon source, 2% casamino acids, and vitamin supplements (0.1 mg/L biotin, 2 mg/L thiamine, 2 mg/L nicotinic acid, 2 mg calcium pantothenate). CDM was prepared with glycerol (5.645 g/L) as the carbon source as previously reported (56), with the following modifications: sodium pantothenate was replaced with calcium pantothenate, FeCl₃ was replaced with FeSO₄ x 7H₂O, and NaCl was added at concentrations stated in the text. In addition, 22 mg/L CaCl₂ x 2H₂O and 10 mg/L MnSO₄ x 4H₂O were added. When appropriate, media were supplemented with antibiotics as listed in Table S2. The methicillin-resistant *S. aureus* (MRSA) strain COL Gateway Clone Set (NR-19277), recombinant in *E. coli* and arrayed in twenty-five 96-well plates, was obtained through BEI Resources, National Institute of Allergy and Infectious Diseases (NIAID), National Institutes of Health (NIH). The library is comprised of 2,343 *E. coli* strains with individual *S. aureus* COL ORFs in the gateway donor vector pDONR221. The construction of the His-MBP fusion protein overproduction library in the gateway destination vector pVL847-Gn (conferring gentamycin resistance; (57)) and introduction into the chloramphenicol resistant *E. coli* protein strain T7IQ is described in Corrigan *et al.*, 2016 (29). The final His-MBP *S. aureus* COL ORF fusion protein overproduction library consisted of 2,337

strains, as 6 gateway reactions were unsuccessful (plate 3 well A3, B7, D2; plate 6 well C2, plate 8 well E1 and plate 19 well D11).

Construction of *E. coli* protein overproduction strains

Primers used for strain and plasmid construction are listed in Table S3. Plasmid pVL847-SACOL2453, from here on out referred to as pVL847-OpuCA was isolated from the original His-MBP *S. aureus* COL ORFeome library strain and retransformed into the *E. coli* strain T71Q to yield strain ANG3128. This strain was used for the production and purification of the His-MBP-OpuCA fusion protein. Plasmid pET28b-CBS was constructed for the production and purification of the His-CBS protein. Primer pair ANG1842/ANG1785 and LAC* genomic DNA were used to amplify the *opuCA* region coding for amino acids 237 to 408 (CBS domain). The resulting PCR product was digested with NheI and EcoRI and inserted into vector pET28b cut with the same enzymes. Plasmid pET28b-CBS was initially recovered in strain XL-1 Blue and subsequently introduced for protein production into strain BL21(DE3), yielding strains ANG3199 and ANG3218, respectively. Plasmids pET28b-CBS^{F283A}, pET28b-CBS^{F294A}, pET28b-CBS^{Y319A}, pET28b-CBS^{Y365A} and pET28b-CBS^{W369A} for the production and purification of the different His-CBS single amino acid substitution variants were constructed by site directed mutagenesis using primer pairs ANG2092/ANG2093, ANG2094/ANG2095, ANG2096/ANG2097, ANG2098/ANG2099, and ANG2100/ANG2101 and plasmid pET28b-CBS from strain ANG3218 as a template. The plasmids were initially recovered in strain XL-1 Blue yielding strains ANG3560 to ANG3564 and subsequently introduced for protein production into strain BL21(DE3) yielding strains ANG3565 to ANG3569. Plasmids pET28b-CBS_{Δ365} and pET28b-CBS^{Δ374} were constructed for the production of C-terminally truncated CBS protein variants lacking amino acids 365-408 or 374-408. The respective *opuCA* fragments were

amplified using the primer ANG1842 and either primer ANG2102 or ANG2103 and *S. aureus* LAC* genomic DNA. The resulting PCR fragment was cut and inserted into the NheI and EcoRI sites of plasmid pET28b. Plasmids pET28b-CBS^{Δ365} and pET28b-CBS^{Δ374} were recovered in *E. coli* XL-1 Blue strains yielding strains ANG3570 and ANG3571 and subsequently introduced into *E. coli* BL21(DE3) giving rise to strains ANG3572 and ANG3573. Plasmid pVL847-ATPase was constructed for the production and purification of the His-MBP-ATPase fusion protein. Primer pair ANG1821/ANG1822 and LAC* genomic DNA were used in a PCR and the resulting product cloned into the XhoI and HindIII sites of vector pVL847. The plasmid pVL847-ATPase was initially recovered in XL-1 Blue and subsequently introduced for protein production and purification into strain BL21(DE3), yielding strains ANG3172 and ANG3173, respectively. Plasmids pVL847-SACOL0762, pVL847-SACOL0921, pVL847-SACOL1013 and pVL847-SACOL1752 were constructed for the production of the CBS domain containing His-MBP fusion proteins either because they were not present in the COL ORF library or in order to remove transmembrane regions that could possibly impede expression and solubility. Of note, while the corresponding genes were amplified from the USA300 strain LAC*, the *S. aureus* strain COL gene nomenclature was used for constancy in naming with the other ORFeome library strains. Primer pairs ANG1923/ANG2363, ANG2364/ANG2365, ANG2366/ANG2367 and ANG1924/ANG1925 and LAC* genomic DNA were used to amplify the respective genes. The resulting PCR products were cut and inserted into the XhoI/BamHI sites of plasmid pVL847. Plasmids pVL847-SACOL0762, pVL847-SACOL0921, pVL847-SACOL1013 and pVL847-SACOL1752 were recovered in *E. coli* strain XL-1 Blue, resulting in strains ANG4046, ANG4047, ANG4048 and ANG3593. The plasmids were then introduced into *E. coli* strain T7IQ for protein production, yielding strains ANG4049, ANG4050, ANG4051, and ANG3597.

The sequences of all inserts were verified by automated fluorescence sequencing at GATC Biotechnology.

***S. aureus* strain constructions**

Plasmid pIMAY Δ *opuCA* was produced for construction of *S. aureus* strains with an in-frame deletion in *opuCA*. To this end, the first 30 bases of *opuCA* plus an approximately 1 kb upstream fragment was amplified with primers ANG2028/ANG2029, and the last 30 bases of *opuCA* plus an approximately 1 kb downstream fragment with primers ANG2030/ANG2031 using LAC* chromosomal DNA. The fragments were fused by splicing overlap extension (SOE) PCR using primers ANG2028 and ANG2031, digested and cloned into EcoRV and NotI sites of plasmid pIMAY. Plasmid pIMAY Δ *opuCA* was recovered in *E. coli* strain XL1-Blue, yielding strain ANG3580, shuttled through *E. coli* strain IM08B (58) yielding strain ANG3728, and subsequently introduced by electroporation into the strain LAC*. The *opuCA* gene was deleted by allelic exchange as previously described (59), yielding the strain LAC* Δ *opuCA* (ANG3744). Successful disruption of *opuCA* was confirmed by PCR. For complementation analysis, the single site integration vector pCL55-*opuCA* was constructed to allow expression of the *opuCA* gene under its native promoter in *S. aureus*. To this end, the *opuCA* gene, including a 643 bp upstream DNA fragment containing the promoter region, was amplified with primer pair ANG2025/ANG2027. The PCR product was partially digested with XmaI as the fragment contained an internal XmaI site and fully digested with EcoRI and inserted into vector pCL55, which had been cut with the same enzymes. The plasmid pCL55-*opuCA* was initially recovered in *E. coli* strain XL1 Blue, yielding strain ANG3581. Next the plasmid was transformed into *E. coli* strain IM08B yielding strain ANG3733 and from there introduced by electroporation into *S.*

aureus strain LAC* Δ *opuCA* (ANG3744) yielding strain LAC* Δ *opuCA* pCL55-*opuCA* (ANG3830). As a control, the empty plasmid vector pCL55 was shuttled through *E. coli* IM08B (ANG3732) and subsequently introduced by electroporation into strains LAC* (ANG1575) and LAC* Δ *opuCA* (ANG3744), yielding strains LAC* pCL55 (ANG3795) and LAC* Δ *opuCA* pCL55 (ANG3829).

Protein purifications and SEC-MALS analysis

Proteins were purified from 1-2 L *E. coli* cultures. Cultures were grown to an OD₆₀₀ of 0.5–0.7 at 37°C, gene expression induced with 0.5 mM IPTG, and cultures incubated overnight at 16°C to 18°C. Protein purifications were performed by nickel affinity and size exclusion chromatography as previously described (16, 60). The His-CBS protein for the protein crystallography work was purified by nickel affinity as described above, however a 20 mM Tris-HCl pH 7.5, 50 mM NaCl, 10 mM MgCl₂ buffer was used for the size exclusion purification step. Protein-containing fractions were combined and concentrated to 10 mg/ml using a 10 kDa cut-off concentrator (Millipore), and protein concentrations were determined by A₂₈₀ readings or using the Pierce BCA protein assay kit. Where indicated, 20 μ l of 5 μ M solution of the purified proteins were also separated on 12% polyacrylamide (PAA) gels and proteins visualized by Coomassie staining. For the SEC-MALS analysis, the purified His-OpuCA protein was adjusted to a concentration of 4 mg/ml in 50mM Tris-HCl pH 7.5, 200mM NaCl, 5% glycerol buffer and loaded on a Superdex 10/300 size exclusion column, which was coupled to a multi-angle laser light scattering detector (Wyatt Technology Corporation). The data were processed with the ASTRA 6.0 software and fitted according to the Zimm model for static light scattering. The analysis was performed three

times with independently purified protein preparations and values from all three experiments are reported.

Protein Crystallization

For crystallization, sitting-drop trials were performed using 1440 different commercially available conditions (Molecular Dimensions and Hampton Research). Plate-shaped crystals appeared after 7-10 days at 4°C under several conditions; the best crystals were obtained with 0.2 M sodium nitrate plus 20% PEG3350. Crystals were flash cooled in liquid nitrogen after serial addition of PEG400 in 10% steps to a final concentration of 30%. The details for structure solution, refinement, and analysis can be found in the supplementary materials and methods section.

Preparation of *E. coli* whole-cell lysates

T7IQ pVL847-Gn *S. aureus* COL ORFeome library strains were grown overnight at 30°C in LB-M9 medium. The following morning, the strains were sub-cultured into fresh LB-M9 medium, grown for 3 h, and gene expression was induced with 1 mM IPTG. Cultures were then incubated for an additional 6 h at 30°C. Bacteria from a 1 ml culture aliquot were collected by centrifugation and suspended in lysis buffer (40 mM Tris (pH 7.5), 100 mM NaCl, 10 mM MgCl₂, 2 mM PMSF, 20 µg/mL DNase, and 0.5 mg/mL lysozyme) in 1/10 of their original volume. Cells were lysed by three freeze-thaw cycles. Lysates were directly used in binding assays or stored frozen. For *E. coli* strains expressing the different *opuCA* variants, the lysates were prepared as described above, but the strains were grown overnight at 30°C in 5 ml of LB medium. Gene expression was then induced by the addition of 1 mM IPTG to the overnight

cultures, incubated for 6 h at 30°C, and cells harvested by centrifugation and suspended to an OD₆₀₀ of 5 in 100 µl lysis buffer.

For testing the capacity of CBS domain-containing proteins to bind c-di-AMP, strains were grown and protein expression induced the same as for the library strains; however lysates were subsequently prepared as follows: Bacteria from 5 ml culture was collected by centrifugation, suspended in 5 ml spheroplasting buffer (50 mM Tris pH 7.5, 20% Sucrose, 5 mM EDTA, 1 mg/ml lysozyme), and incubated on ice for 20 min. Spheroplasts were collected by 10 min low-speed centrifugation at 180 x g, the supernatant removed, and cells subsequently lysed by vigorously suspending in 1 ml of cold lysis buffer (5mM Tris pH 7.5). Then DNase I (50 µg/ml) and MgCl (20 mM MgCl) were added and the lysate incubated at room temperature for 30 min. The lysate was either used directly for nucleotide binding assays or following removal of insoluble proteins by centrifugation at 4 °C for 1 h at 21,000 x g.

Differential radial capillary action of ligand assay (DRaCALA)

The principle of the DRaCALA is described in Roelofs *et al.* (30) and has been adapted for the study of c-di-AMP binding proteins by Corrigan *et al.* (16). Briefly, 9 µl of *E. coli* whole-cell lysates in binding buffer were mixed with ~1 nM ³²P-labeled c-di-AMP, which was synthesized in vitro as previously described using the *Bacillus thuringiensis* DisA enzyme (18). The reactions were incubated at room temperature for 5 min and 2.5 µl were spotted onto nitrocellulose membranes. For the whole-genome screen, the ³²P-labeled c-di-AMP was dispensed into 96-well plates containing 20 µl lysates and subsequently spotted onto nitrocellulose membrane using a 96-well pin tool (V&P Scientific). Membranes were placed into cassettes with phosphor screens, and the signal was visualized using a Typhoon 7000 (GE Healthcare). For competition assays, 10

μM of purified protein was mixed with $100 \mu\text{M}$ of the different cold nucleotides [AMP, ADP, ATP, GTP (Sigma); cAMP, cGMP, pApA (Biolog); c-di-AMP, c-di-GMP (Invivogen)] and $2.5 \mu\text{l}$ of the reaction mixtures were spotted onto nitrocellulose membranes. For DRaCALAs with purified protein, $10 \mu\text{M}$ protein solutions in binding buffer were mixed with $\sim 1 \text{ nM}$ ^{32}P -labeled c-di-AMP. For K_d analysis, two-fold dilutions of purified protein solutions giving final concentrations ranging from $100 \mu\text{M}$ to $0.1 \mu\text{M}$ or $50 \mu\text{M}$ to $0.1 \mu\text{M}$ in binding buffer were mixed with $\sim 1 \text{ nM}$ ^{32}P -labeled c-di-AMP. For all assays, the purified proteins were incubated with the radiolabelled c-di-AMP for 5 min at RT. $2.5 \mu\text{l}$ of these reaction mixtures were then spotted onto nitrocellulose membranes, air-dried, and radioactivity signals detected as described above. The fraction of ligand bound and as previously described (30) and the K_d values determined using a non-linear regression with Hill coefficient ($Y = B_{\text{max}} * X^h / (K_d^h + X^h)$).

Uptake of radiolabeled compatible solutes

The uptake of radiolabeled glycine betaine, choline chloride, and carnitine hydrochloride was measured using a previously described method (61, 62) with the following modifications: *S. aureus* strains were grown overnight in CDM with 0.5 M NaCl and the cultures back-diluted the following morning to an OD_{600} of 0.2 OD in 20 ml of CDM with 0.5 M NaCl . Because not all strains could be processed at once, cultures were inoculated in a staggered fashion one hour apart. The cultures were then grown at 37°C to exponential phase ($\text{OD}_{600} \sim 0.5$), at which point a culture equivalent of $\text{OD} = 8$ was removed and bacteria collected by centrifugation at $8000 \times g$ for 10 min. The supernatants were removed and the cell pellets suspended in 4 ml CDM with 0.5 M NaCl . Then the OD was measured and the cell density adjusted to an $\text{OD}_{600} = 1$. Before the radiolabeled compound was added, an initial $100 \mu\text{l}$ aliquot of this cell suspension was applied to

a 0.2 μm cellulose nitrate membrane (Millipore), vacuum-filtered, and washed with 17 ml of CDM containing 0.5 M NaCl. This sample was used as a measure of background radiation in the experimental system. To measure uptake of radiolabeled compounds, betaine [glycine-1- ^{14}C] (Hartmann Analytic), choline chloride [methyl- ^{14}C] (PerkinElmer), or carnitine hydrochloride L-[N-methyl- ^{14}C] (Hartmann Analytic) was added to a final concentration of 25 μM (0.046 MBq / 1.25 μCi) to the remaining 900 μl of the cell suspension. At 0, 3, and 6 minutes, and in some cases every minute, 100 μl aliquots were removed, filtered, and washed with 17 ml of CDM with 0.5 M NaCl. The membrane filters were added to 9 ml of Filter-Count scintillation fluid (PerkinElmer) and radioactivity measured in counts per minute (CPM) using a Wallac 1409 DSA liquid scintillation counter. The long-term carnitine uptake experiment with the LAC* wild-type and ΔgdpP strains was done as described above with the following changes: chloramphenicol (100 $\mu\text{g/ml}$) was added to the cell suspensions after their harvest to minimize growth. An initial aliquot of 400 μl was removed and 50 μl , instead of 100 μl aliquots, were taken for the radioactive uptake measurements. The cells were then incubated at 37°C with shaking. In addition, a culture treated identically, but without the addition of radiolabeled carnitine, was used to measure at each time point the OD_{600} to adjust for slight differences in residual growth, which occurred despite the addition of chloramphenicol.

Choline uptake assays were conducted as described by Kiran *et al.* (37). *S. aureus* cultures were grown overnight in M9 medium containing glucose, casamino acids, and vitamins. The next day, the cultures were back-diluted to an OD_{600} of 0.01 into the same medium and grown until they reached an OD_{600} of 0.2. Next, 2 ml aliquots were transferred to conical tubes and 200 μl of the cultures filtered to determine the background radioactivity. Radiolabeled choline was added to the remaining culture to a final concentration of 5 μM (0.0102 MBq / 0.2757 μCi). 200 μl

samples were filtered at 0, 3 and 6 minutes, washed with 20 ml 0.1 x PBS, and the radioactivity on the filter was determined using a scintillation counter.

Detection of OpuCA by western blot

For the detection of the *S. aureus* OpuCA protein by western blot, a polyclonal rabbit antibody was generated at Covalab using the purified His-CBS proteins (OpuCA aa 207-408) as immunogen. Samples for western blot analysis were prepared from *S. aureus* strains LAC* pCL55, LAC* Δ opuCA pCL55 and the LAC* Δ opuCA pCL55-opuCA as described previously (7), with small modifications. Briefly, bacteria from 1 ml *S. aureus* culture were collected by centrifugation (13,000 x g, 5 min) and suspended per OD₆₀₀ unit in 15 μ l of 50 mM Tris-HCl, pH 7.5, 10 mM MgCl₂ buffer containing 100 μ g/ml lysostaphin and 20 μ g/ml DNase A. The samples were incubated for 30 min at 37°C, an equal volume of 2x SDS protein sample loading buffer was added and the samples were subsequently boiled for 15 mins. 10 μ l samples were loaded on a 12% SDS-polyacrylamide gel and proteins separated by electrophoresis, followed by electro-transfer onto PVDF membranes. Western-blots were performed using the OpuCA antibody (Covalab) and an HRP-conjugated antibody recognizing rabbit IgG (Cell signaling technology) at 1:10,000 dilutions. Blots were developed using the Clarity ECL substrate (BioRad) and visualized using the ChemiDoc Touch Imaging System (BioRad).

Statistical analyses

Statistical analyses were done using Prism version 6.0f (Graphpad) and a Kruskal-Wallis test followed by a Dunn's multiple comparison test was performed on the data sets as indicated in

each legend. Adjusted p-values < 0.01 are indicated by double asterisk (**) and p-values <0.05 by a single asterisk (*).

SUPPLEMENTARY MATERIALS

Supplemental Materials and Methods

Fig. S1. Identification of SACOL2453 (OpuCA) as a potential c-di-AMP target protein using a genome wide DRaCALA screen

Fig. S2. DRaCALAs with cleared cell lysates derived from *E. coli* strains producing different CBS domain–containing *S. aureus* proteins.

Fig. S3. Oligomeric state of the *S. aureus* OpuCA CBS domain in the crystal structure and in solution

Fig. S4. Structure-based sequence alignment of the *S. aureus* OpuCA CBS domain with other ligand-bound CBS domains

Fig. S5. OpuCA protein amounts in wild-type *S. aureus*, mutant, and complementation strains

Fig. S6. Confirmed and putative osmolyte uptake systems in *S. aureus* strains

Tables S1. Data collection and refinement statistics (molecular replacement)

Tables S2. Bacterial strains used in this study

Tables S3. Primers used in this study

REFERENCES AND NOTES

1. U. Römling, Great times for small molecules: c-di-AMP, a second messenger candidate in Bacteria and Archaea. *Sci Signal* **1**, pe39 (2008).

2. R. M. Corrigan, A. Gründling, Cyclic di-AMP: another second messenger enters the fray. *Nat Rev Microbiol* **11**, 513-524 (2013).
3. G. Witte, S. Hartung, K. Buttner, K. P. Hopfner, Structural biochemistry of a bacterial checkpoint protein reveals diadenylate cyclase activity regulated by DNA recombination intermediates. *Mol Cell* **30**, 167-178 (2008).
4. F. Rao, R. Y. See, D. Zhang, D. C. Toh, Q. Ji, Z. X. Liang, YybT is a signaling protein that contains a cyclic dinucleotide phosphodiesterase domain and a GGDEF domain with ATPase activity. *J Biol Chem* **285**, 473-482 (2010).
5. T. N. Huynh, S. Luo, D. Pensinger, J. D. Sauer, L. Tong, J. J. Woodward, An HD-domain phosphodiesterase mediates cooperative hydrolysis of c-di-AMP to affect bacterial growth and virulence. *Proc Natl Acad Sci U S A* **112**, E747-756 (2015).
6. R. M. Corrigan, J. C. Abbott, H. Burhenne, V. Kaefer, A. Gründling, c-di-AMP is a new second messenger in *Staphylococcus aureus* with a role in controlling cell size and envelope stress. *PLoS Pathog* **7**, e1002217 (2011).
7. R. M. Corrigan, L. Bowman, A. R. Willis, V. Kaefer, A. Gründling, Cross-talk between two nucleotide-signaling pathways in *Staphylococcus aureus*. *J Biol Chem* **290**, 5826-5839 (2015).
8. V. Dengler, N. McCallum, P. Kiefer, P. Christen, A. Patrignani, J. A. Vorholt, B. Berger-Bächi, M. M. Senn, Mutation in the C-di-AMP cyclase *dacA* affects fitness and resistance of methicillin resistant *Staphylococcus aureus*. *PLoS One* **8**, e73512 (2013).
9. T. N. Huynh, J. J. Woodward, Too much of a good thing: regulated depletion of c-di-AMP in the bacterial cytoplasm. *Curr Opin Microbiol* **30**, 22-29 (2016).

10. F. M. Mehne, K. Gunka, H. Eilers, C. Herzberg, V. Kaefer, J. Stülke, Cyclic di-AMP homeostasis in bacillus subtilis: both lack and high level accumulation of the nucleotide are detrimental for cell growth. *J Biol Chem* **288**, 2004-2017 (2013).
11. J. J. Woodward, A. T. Iavarone, D. A. Portnoy, c-di-AMP secreted by intracellular *Listeria monocytogenes* activates a host type I interferon response. *Science* **328**, 1703-1705 (2010).
12. A. T. Whiteley, A. J. Pollock, D. A. Portnoy, The PAMP c-di-AMP Is Essential for *Listeria monocytogenes* Growth in Rich but Not Minimal Media due to a Toxic Increase in (p)ppGpp. *Cell Host Microbe* **17**, 788-798 (2015).
13. K. Sureka, P. H. Choi, M. Precit, M. Delince, D. A. Pensinger, T. N. Huynh, A. R. Jurado, Y. A. Goo, M. Sadilek, A. T. Iavarone, J. D. Sauer, L. Tong, J. J. Woodward, The cyclic dinucleotide c-di-AMP is an allosteric regulator of metabolic enzyme function. *Cell* **158**, 1389-1401 (2014).
14. T. N. Huynh, P. H. Choi, K. Sureka, H. E. Ledvina, J. Campillo, L. Tong, J. J. Woodward, Cyclic di-AMP targets the cystathionine beta-synthase domain of the osmolyte transporter OpuC. *Mol Microbiol*, (2016). Jul 5. doi: 10.1111/mmi.13456.
15. L. Zhang, W. Li, Z. G. He, DarR, a TetR-like transcriptional factor, is a cyclic di-AMP-responsive repressor in *Mycobacterium smegmatis*. *J Biol Chem* **288**, 3085-3096 (2013).
16. R. M. Corrigan, I. Campeotto, T. Jeganathan, K. G. Roelofs, V. T. Lee, A. Gründling, Systematic identification of conserved bacterial c-di-AMP receptor proteins. *Proc Natl Acad Sci U S A* **110**, 9084-9089 (2013).
17. J. Gundlach, A. Dickmanns, K. Schröder-Tittmann, P. Neumann, J. Kaesler, J. Kampf, C. Herzberg, E. Hammer, F. Schwede, V. Kaefer, K. Tittmann, J. Stülke, R. Ficner,

- Identification, characterization, and structure analysis of the cyclic di-AMP-binding PII-like signal transduction protein DarA. *J Biol Chem* **290**, 3069-3080 (2015).
18. I. Campeotto, Y. Zhang, M. G. Mladenov, P. S. Freemont, A. Gründling, Complex structure and biochemical characterization of the *Staphylococcus aureus* cyclic diadenylate monophosphate (c-di-AMP)-binding protein PstA, the founding member of a new signal transduction protein family. *J Biol Chem* **290**, 2888-2901 (2015).
 19. M. Müller, K. P. Hopfner, G. Witte, c-di-AMP recognition by *Staphylococcus aureus* PstA. *FEBS Lett* **589**, 45-51 (2015).
 20. P. H. Choi, K. Sureka, J. J. Woodward, L. Tong, Molecular basis for the recognition of cyclic-di-AMP by PstA, a PII-like signal transduction protein. *Microbiologyopen* **4**, 361-374 (2015).
 21. J. A. Moscoso, H. Schramke, Y. Zhang, T. Tosi, A. Dehbi, K. Jung, A. Gründling, Binding of Cyclic Di-AMP to the *Staphylococcus aureus* Sensor Kinase KdpD Occurs via the Universal Stress Protein Domain and Downregulates the Expression of the Kdp Potassium Transporter. *J Bacteriol* **198**, 98-110 (2015).
 22. Y. Bai, J. Yang, T. M. Zarrella, Y. Zhang, D. W. Metzger, G. Bai, Cyclic di-AMP impairs potassium uptake mediated by a cyclic di-AMP binding protein in *Streptococcus pneumoniae*. *J Bacteriol* **196**, 614-623 (2014).
 23. H. Kim, S. J. Youn, S. O. Kim, J. Ko, J. O. Lee, B. S. Choi, Structural Studies of Potassium Transport Protein KtrA Regulator of Conductance of K⁺ (RCK) C Domain in Complex with Cyclic Diadenosine Monophosphate (c-di-AMP). *J Biol Chem* **290**, 16393-16402 (2015).

24. K. H. Chin, J. M. Liang, J. G. Yang, M. S. Shih, Z. L. Tu, Y. C. Wang, X. H. Sun, N. J. Hu, Z. X. Liang, J. M. Dow, R. P. Ryan, S. H. Chou, Structural Insights into the Distinct Binding Mode of Cyclic Di-AMP with SaCpaA_RCK. *Biochemistry* **54**, 4936-4951 (2015).
25. T. A. Krulwich, D. B. Hicks, M. Ito, Cation/proton antiporter complements of bacteria: why so large and diverse? *Mol Microbiol* **74**, 257-260 (2009).
26. W. Epstein, The roles and regulation of potassium in bacteria. *Prog Nucleic Acid Res Mol Biol* **75**, 293-320 (2003).
27. J. M. Wood, Bacterial osmoregulation: a paradigm for the study of cellular homeostasis. *Annu Rev Microbiol* **65**, 215-238 (2011).
28. J. M. Wood, E. Bremer, L. N. Csonka, R. Kraemer, B. Poolman, T. van der Heide, L. T. Smith, Osmosensing and osmoregulatory compatible solute accumulation by bacteria. *Comp Biochem Physiol A Mol Integr Physiol* **130**, 437-460 (2001).
29. R. M. Corrigan, L. E. Bellows, A. Wood, A. Gründling, ppGpp negatively impacts ribosome assembly affecting growth and antimicrobial tolerance in Gram-positive bacteria. *Proc Natl Acad Sci U S A*, (2016).
30. K. G. Roelofs, J. Wang, H. O. Sintim, V. T. Lee, Differential radial capillary action of ligand assay for high-throughput detection of protein-metabolite interactions. *Proc. Natl. Acad. Sci. U S A* **108**, 15528-15533 (2011).
31. J. Ereno-Orbea, T. Majtan, I. Oyenarte, J. P. Kraus, L. A. Martinez-Cruz, Structural basis of regulation and oligomerization of human cystathionine beta-synthase, the central enzyme of transsulfuration. *Proc Natl Acad Sci U S A* **110**, E3790-3799 (2013).

32. E. Krissinel, K. Henrick, Inference of macromolecular assemblies from crystalline state. *J Mol Biol* **372**, 774-797 (2007).
33. E. Krissinel, K. Henrick, Secondary-structure matching (SSM), a new tool for fast protein structure alignment in three dimensions. *Acta Crystallogr D Biol Crystallogr* **60**, 2256-2268 (2004).
34. M. Lucas, J. A. Encinar, E. A. Arribas, I. Oyenarte, I. G. Garcia, D. Kortazar, J. A. Fernandez, J. M. Mato, M. L. Martinez-Chantar, L. A. Martinez-Cruz, Binding of S-methyl-5'-thioadenosine and S-adenosyl-L-methionine to protein MJ0100 triggers an open-to-closed conformational change in its CBS motif pair. *J Mol Biol* **396**, 800-820 (2010).
35. J. Ereno-Orbea, I. Oyenarte, L. A. Martinez-Cruz, CBS domains: Ligand binding sites and conformational variability. *Arch Biochem Biophys* **540**, 70-81 (2013).
36. N. A. Baker, D. Sept, S. Joseph, M. J. Holst, J. A. McCammon, Electrostatics of nanosystems: application to microtubules and the ribosome. *Proc Natl Acad Sci U S A* **98**, 10037-10041 (2001).
37. M. D. Kiran, D. E. Akiyoshi, A. Giacometti, O. Cirioni, G. Scalise, N. Balaban, OpuC-- an ABC transporter that is associated with *Staphylococcus aureus* pathogenesis. *Int J Artif Organs* **32**, 600-610 (2009).
38. R. M. Kappes, B. Kempf, E. Bremer, Three transport systems for the osmoprotectant glycine betaine operate in *Bacillus subtilis*: characterization of OpuD. *J Bacteriol* **178**, 5071-5079 (1996).

39. A. S. Angelidis, G. M. Smith, Three transporters mediate uptake of glycine betaine and carnitine by *Listeria monocytogenes* in response to hyperosmotic stress. *Appl Environ Microbiol* **69**, 1013-1022 (2003).
40. C. M. Gries, J. L. Bose, A. S. Nuxoll, P. D. Fey, K. W. Bayles, The Ktr potassium transport system in *Staphylococcus aureus* and its role in cell physiology, antimicrobial resistance and pathogenesis. *Mol Microbiol* **89**, 760-773 (2013).
41. A. Price-Whelan, C. K. Poon, M. A. Benson, T. T. Eidem, C. M. Roux, J. M. Boyd, P. M. Dunman, V. J. Torres, T. A. Krulwich, Transcriptional profiling of *Staphylococcus aureus* during growth in 2 M NaCl leads to clarification of physiological roles for Kdp and Ktr K⁺ uptake systems. *MBio* **4**, (2013).
42. B. Kempf, E. Bremer, Uptake and synthesis of compatible solutes as microbial stress responses to high-osmolality environments. *Arch Microbiol* **170**, 319-330 (1998).
43. E. Bremer, R. Krämer, in *Bacterial stress responses*, G. Storz, R. Hengge-Aronis, Eds. (ASM Press, Washington, DC., 2000), pp. 79-97.
44. K. J. Wetzel, D. Bjorge, W. R. Schwan, Mutational and transcriptional analyses of the *Staphylococcus aureus* low-affinity proline transporter OpuD during in vitro growth and infection of murine tissues. *FEMS Immunol Med Microbiol* **61**, 346-355 (2011).
45. W. R. Schwan, L. Lehmann, J. McCormick, Transcriptional activation of the *Staphylococcus aureus* *putP* gene by low-proline-high osmotic conditions and during infection of murine and human tissues. *Infect Immun* **74**, 399-409 (2006).
46. E. Biemans-Oldehinkel, N. A. Mahmood, B. Poolman, A sensor for intracellular ionic strength. *Proc Natl Acad Sci U S A* **103**, 10624-10629 (2006).

47. N. A. Mahmood, E. Biemans-Oldehinkel, J. S. Patzlaff, G. K. Schuurman-Wolters, B. Poolman, Ion specificity and ionic strength dependence of the osmoregulatory ABC transporter OpuA. *J Biol Chem* **281**, 29830-29839 (2006).
48. N. A. Mahmood, E. Biemans-Oldehinkel, B. Poolman, Engineering of ion sensing by the cystathionine beta-synthase module of the ABC transporter OpuA. *J Biol Chem* **284**, 14368-14376 (2009).
49. S. Ignoul, J. Eggermont, CBS domains: structure, function, and pathology in human proteins. *Am J Physiol Cell Physiol* **289**, C1369-1378 (2005).
50. W. M. Smith, T. H. Pham, L. Lei, J. Dou, A. H. Soomro, S. A. Beatson, G. A. Dykes, M. S. Turner, Heat resistance and salt hypersensitivity in *Lactococcus lactis* due to spontaneous mutation of limg_1816 (*gdpP*) induced by high-temperature growth. *Appl Environ Microbiol* **78**, 7753-7759 (2012).
51. C. E. Witte, A. T. Whiteley, T. P. Burke, J. D. Sauer, D. A. Portnoy, J. J. Woodward, Cyclic di-AMP is critical for *Listeria monocytogenes* growth, cell wall homeostasis, and establishment of infection. *MBio* **4**, e00282-00213 (2013).
52. F. Rallu, A. Gruss, S. D. Ehrlich, E. Maguin, Acid- and multistress-resistant mutants of *Lactococcus lactis* : identification of intracellular stress signals. *Mol Microbiol* **35**, 517-528 (2000).
53. C. Pozzi, E. M. Waters, J. K. Rudkin, C. R. Schaeffer, A. J. Lohan, P. Tong, B. J. Loftus, G. B. Pier, P. D. Fey, R. C. Massey, J. P. O'Gara, Methicillin resistance alters the biofilm phenotype and attenuates virulence in *Staphylococcus aureus* device-associated infections. *PLoS Pathog* **8**, e1002626 (2012).

54. J. M. Griffiths, A. J. O'Neill, Loss of function of the *gdpP* protein leads to joint beta-lactam/glycopeptide tolerance in *Staphylococcus aureus*. *Antimicrob Agents Chemother* **56**, 579-581 (2012).
55. H. O. Smith, M. Levine, Two Sequential Repressions of DNA Synthesis in the Establishment of Lysogeny by Phage P22 and Its Mutants. *Proc Natl Acad Sci U S A* **52**, 356-363 (1964).
56. D. E. Townsend, B. J. Wilkinson, Proline transport in *Staphylococcus aureus*: a high-affinity system and a low-affinity system involved in osmoregulation. *J Bacteriol* **174**, 2702-2710 (1992).
57. K. G. Roelofs, C. J. Jones, S. R. Helman, X. Shang, M. W. Orr, J. R. Goodson, M. Y. Galperin, F. H. Yildiz, V. T. Lee, Systematic Identification of Cyclic-di-GMP Binding Proteins in *Vibrio cholerae* Reveals a Novel Class of Cyclic-di-GMP-Binding ATPases Associated with Type II Secretion Systems. *PLoS Pathog* **11**, e1005232 (2015).
58. I. R. Monk, J. J. Tree, B. P. Howden, T. P. Stinear, T. J. Foster, Complete Bypass of Restriction Systems for Major *Staphylococcus aureus* Lineages. *MBio* **6**, e00308-00315 (2015).
59. I. R. Monk, I. M. Shah, M. Xu, M. W. Tan, T. J. Foster, Transforming the untransformable: application of direct transformation to manipulate genetically *Staphylococcus aureus* and *Staphylococcus epidermidis*. *MBio* **3**, (2012).
60. D. Lu, M. E. Wörmann, X. Zhang, O. Schneewind, A. Gründling, P. S. Freemont, Structure-based mechanism of lipoteichoic acid synthesis by *Staphylococcus aureus* LtaS. *Proc Natl Acad Sci U S A* **106**, 1584-1589 (2009).

61. J. Boch, B. Kempf, E. Bremer, Osmoregulation in *Bacillus subtilis*: synthesis of the osmoprotectant glycine betaine from exogenously provided choline. *J Bacteriol* **176**, 5364-5371 (1994).
62. K. R. Fraser, D. Harvie, P. J. Coote, C. P. O'Byrne, Identification and characterization of an ATP binding cassette L-carnitine transporter in *Listeria monocytogenes*. *Appl Environ Microbiol* **66**, 4696-4704 (2000).
63. G. Winter, C. M. Lobley, S. M. Prince, Decision making in xia2. *Acta Crystallogr D Biol Crystallogr* **69**, 1260-1273 (2013).
64. W. Kabsch, Xds. *Acta Crystallogr D* **66**, 125-132 (2010).
65. M. D. Winn, C. C. Ballard, K. D. Cowtan, E. J. Dodson, P. Emsley, P. R. Evans, R. M. Keegan, E. B. Krissinel, A. G. Leslie, A. McCoy, S. J. McNicholas, G. N. Murshudov, N. S. Pannu, E. A. Potterton, H. R. Powell, R. J. Read, A. Vagin, K. S. Wilson, Overview of the CCP4 suite and current developments. *Acta Crystallogr D Biol Crystallogr* **67**, 235-242 (2011).
66. P. D. Adams, P. V. Afonine, G. Bunkoczi, V. B. Chen, I. W. Davis, N. Echols, J. J. Headd, L. W. Hung, G. J. Kapral, R. W. Grosse-Kunstleve, A. J. McCoy, N. W. Moriarty, R. Oeffner, R. J. Read, D. C. Richardson, J. S. Richardson, T. C. Terwilliger, P. H. Zwart, PHENIX: a comprehensive Python-based system for macromolecular structure solution. *Acta Crystallogr D* **66**, 213-221 (2010).
67. F. DiMaio, Advances in Rosetta structure prediction for difficult molecular-replacement problems. *Acta Crystallogr D Biol Crystallogr* **69**, 2202-2208 (2013).
68. D. E. Kim, D. Chivian, D. Baker, Protein structure prediction and analysis using the Robetta server. *Nucleic Acids Res* **32**, W526-531 (2004).

69. A. J. McCoy, R. W. Grosse-Kunstleve, P. D. Adams, M. D. Winn, L. C. Storoni, R. J. Read, Phaser crystallographic software. *Journal of applied crystallography* **40**, 658-674 (2007).
70. A. A. Vagin, R. A. Steiner, A. A. Lebedev, L. Potterton, S. McNicholas, F. Long, G. N. Murshudov, REFMAC5 dictionary: organization of prior chemical knowledge and guidelines for its use. *Acta crystallographica. Section D, Biological crystallography* **60**, 2184-2195 (2004).
71. P. Emsley, B. Lohkamp, W. G. Scott, K. Cowtan, Features and development of Coot. *Acta Crystallogr D* **66**, 486-501 (2010).
72. V. B. Chen, W. B. Arendall, 3rd, J. J. Headd, D. A. Keedy, R. M. Immormino, G. J. Kapral, L. W. Murray, J. S. Richardson, D. C. Richardson, MolProbity: all-atom structure validation for macromolecular crystallography. *Acta Crystallogr D Biol Crystallogr* **66**, 12-21 (2010).
73. T. J. Dolinsky, P. Czodrowski, H. Li, J. E. Nielsen, J. H. Jensen, G. Klebe, N. A. Baker, PDB2PQR: expanding and upgrading automated preparation of biomolecular structures for molecular simulations. *Nucleic Acids Res* **35**, W522-525 (2007).
74. C. Gille, C. Frommel, STRAP: editor for STRuctural Alignments of Proteins. *Bioinformatics* **17**, 377-378 (2001).
75. C. Y. Lee, S. L. Buranen, Z. H. Ye, Construction of single-copy integration vectors for *Staphylococcus aureus*. *Gene* **103**, 101-105 (1991).
76. V. T. Lee, J. M. Matewish, J. L. Kessler, M. Hyodo, Y. Hayakawa, S. Lory, A cyclic-di-GMP receptor required for bacterial exopolysaccharide production. *Mol. Microbiol.* **65**, 1474-1484 (2007).

77. B. R. Boles, M. Thoendel, A. J. Roth, A. R. Horswill, Identification of genes involved in polysaccharide-independent *Staphylococcus aureus* biofilm formation. *PLoS One* **5**, e10146 (2010).

Acknowledgements: Funding: This work was supported by the European Research Council grant 260371 and the Wellcome Trust grant 100289 to A.G and the German research foundation (DFG) grant SCHU 3159/1-1 to C.F.S. **Author contributions:** C.F.S, L.E.B, T.T, I.C, and A.G, designed the experiment, C.F.S, L.E.B, T.T, I.C, performed experiments; L.E.B, C.F.S., T.T., I.C., R.C., P.F. and A.G. analyzed the data, C.F.S, T.T, and A.G wrote the manuscript.

Competing interests: The authors do not have a conflict of interest to declare. **Data and materials availability:** The coordinates of the OpuCA CBS domain have been deposited in the Protein Database, under PDB code 5IIP.

FIGURE LEGENDS

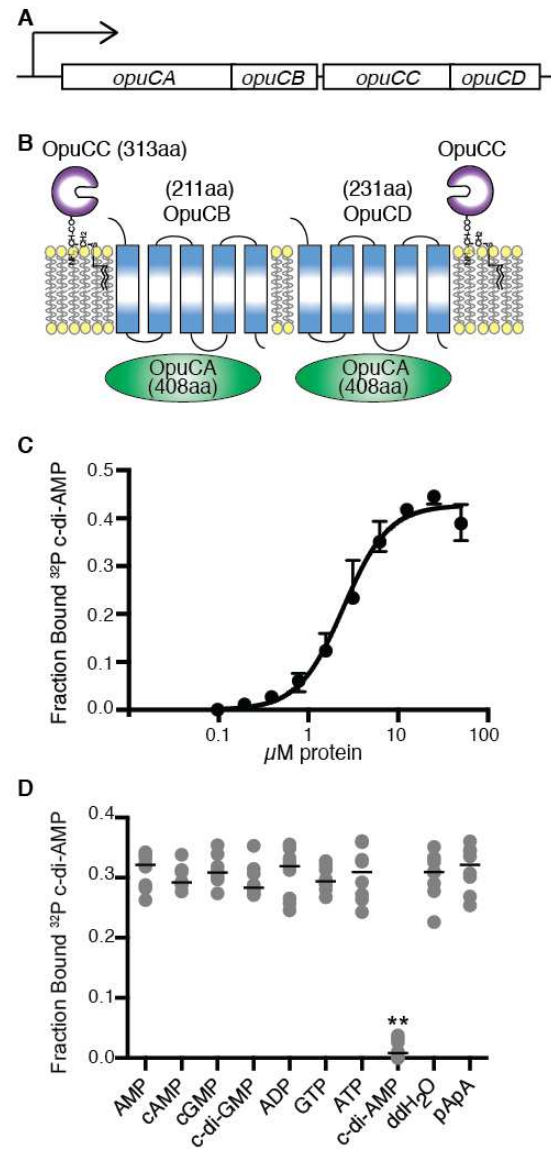


Fig. 1. c-di-AMP interacts specifically and with physiological strength with OpuCA.

Schematic representations of (A) the *opuCA-opuCD* operon structure and (B) the OpuC ATP-binding cassette osmoprotectant uptake system. (C) Binding curve and K_d determination between c-di-AMP and OpuCA. Radiolabeled c-di-AMP and purified His-MBP-OpuCA protein were used in DRaCALAs, the median fraction bound values and ranges were plotted, and the curve fitted and K_d value determined using a non-linear equation with hill coefficient ($n=4$, two independent protein purifications). (D) Nucleotide binding competition assays. Purified His-MBP-OpuCA was incubated with radiolabeled 1 nM c-di-AMP and 100 μ M unlabelled competitor nucleotide. The median fraction bound values and ranges were determined and plotted ($n=8$, two independent protein purifications). Statistical analysis was done using a Kruskal-Wallis test, followed by Dunn's multiple comparison test. Adjusted p-values < 0.01 are indicated by double asterisk (**).

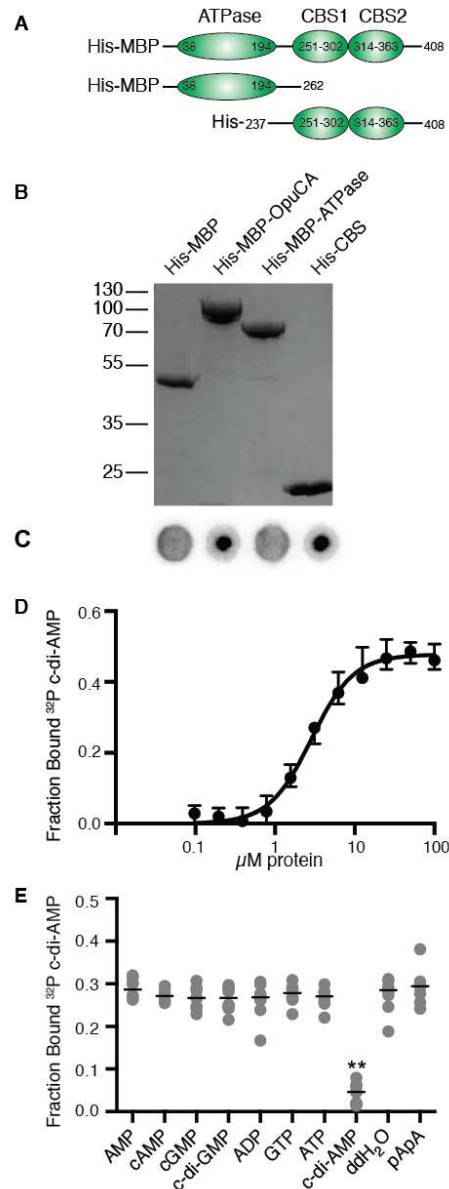


Fig. 2. c-di-AMP interacts specifically with the CBS pair domain of OpuCA. (A) Schematic representation of the full-length His-MBP-OpuCA (top), His-MBP-ATPase (middle) and His-CBS (bottom) fusion proteins. (B) Coomassie stained gel showing the purified fusion proteins indicated above each lane (n=2, two independent protein purifications). (C) DRaCALA spots. The purified proteins shown in (B) were mixed with radiolabeled c-di-AMP and spotted onto nitrocellulose membranes. Spots were visualized using a phosphor imager (n=2, two independent protein purifications). (D) Binding curve and K_d determination. Radiolabeled c-di-AMP and purified His-CBS protein were used in DRaCALAs and K_d value determined using a non-linear equation with hill coefficient (n=5, two independent protein purifications). (E) Nucleotide binding competition assays. Competition assays were performed as described for Figure 1 (n=8, two independent protein purifications). Statistical analysis was first done using a Kruskal-Wallis test, followed by Dunn's multiple comparison test. Adjusted p-values < 0.01 are indicated by double asterisk (**).

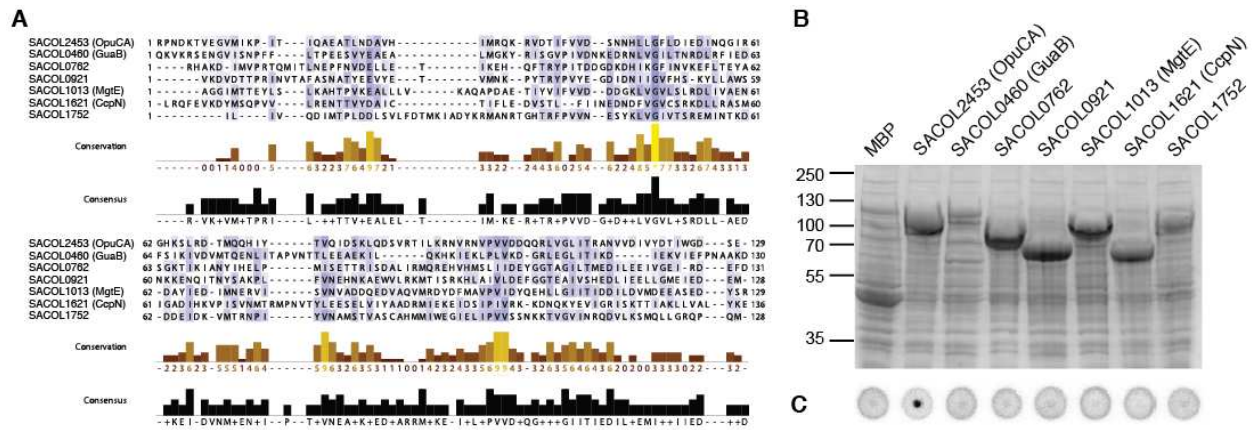


Fig. 3. c-di-AMP does not bind to other *S. aureus* CBS domain containing proteins. (A) ClustalW alignments of the CBS domains found in the seven different *S. aureus* proteins. Only the CBS domain pair region plus 10 amino acids flanking each end was used for the alignment. (B) Coomassie stained gel showing lysates from *E. coli* strains overproducing the His-MBP control protein (lane 1) or His-MBP-fusion to the *S. aureus* protein indicated above each of the other lanes were separated on a polyacrylamide gel and visualized by Coomassie staining (n=4). For the membrane proteins SACOL0762, SACOL0921, and SACOL1013, His-MBP fusion proteins to the CBS domain only, but lacking the transmembrane regions, were used. (C) Representative DRaCALA assays showing lysates analyzed in panel (B) plus with radiolabeled c-di-AMP (n=4).

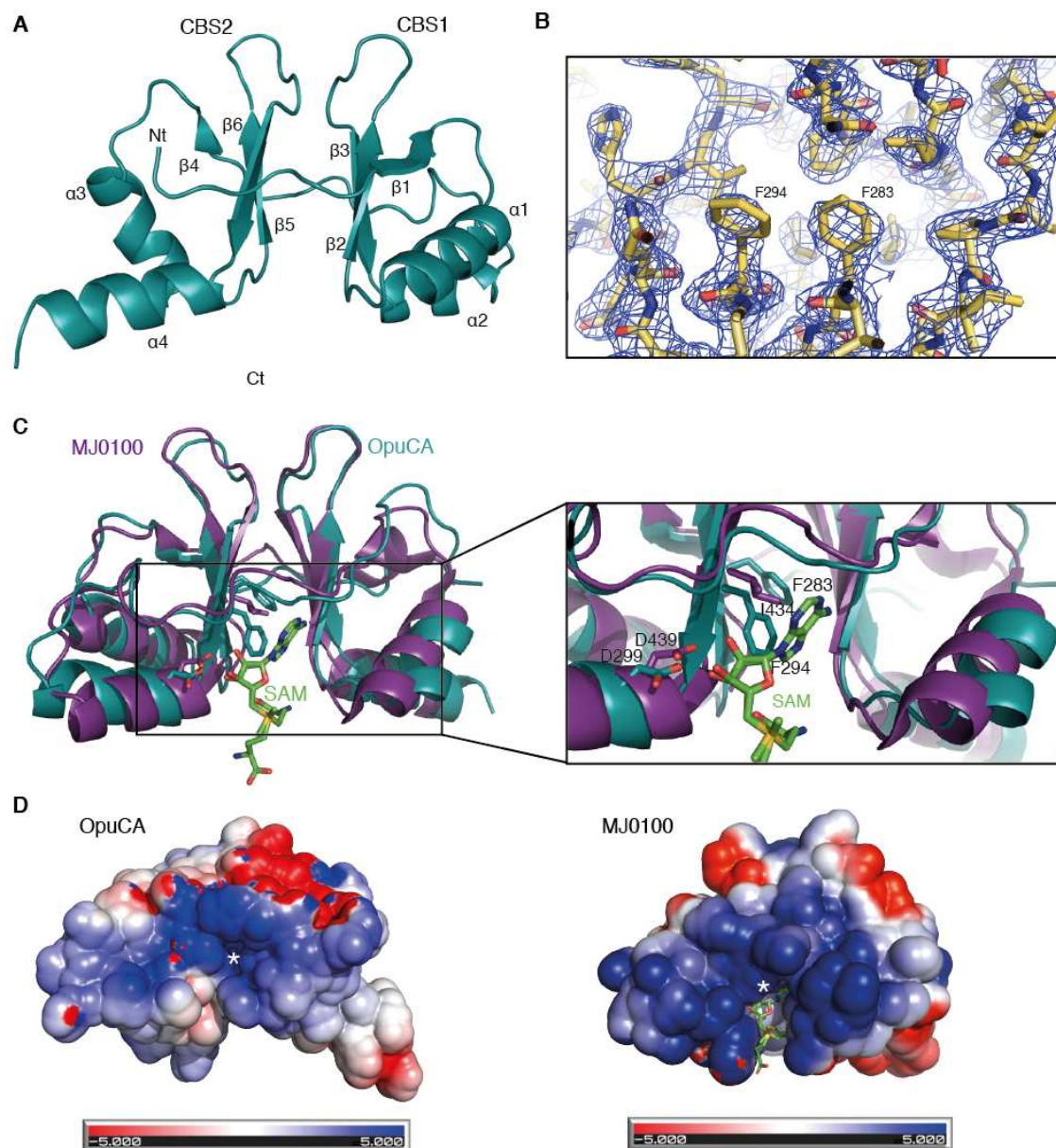


Fig. 4. Structure of the *S. aureus* OpuCA CBS domain and putative c-di-AMP binding site. (A) Crystal structure of a monomer of the *S. aureus* OpuCA CBS domain. (B) Sample of the electron density map showing the potential c-di-AMP binding site. (C) Overlay of the *S. aureus* OpuCA CBS domain (green) and the *M. jannaschii* MJ0100 protein (purple) (rmsd = 1.7 Å). The SAM ligand in the MJ0100 protein is depicted in light green. A close-up view of the SAM binding site is shown on the right. The side chains of Asp⁴³⁹ and Ile⁴³⁴ in MJ0100, which are involved in SAM binding, and the side chains of Phe²⁸³ and Phe²⁹⁴ in OpuCA, which are putatively involved in c-di-AMP binding, are shown as sticks. (D) Electrostatic surface analysis of the *S. aureus* OpuCA CBS domains (left) and the SAM-bound MJ0100 protein (right). Positively and negatively charged areas are coloured in blue and red, respectively. The putative c-di-AMP binding groove in OpuCA and the SAM binding region in MJ0100 are marked with white asterisks (*).

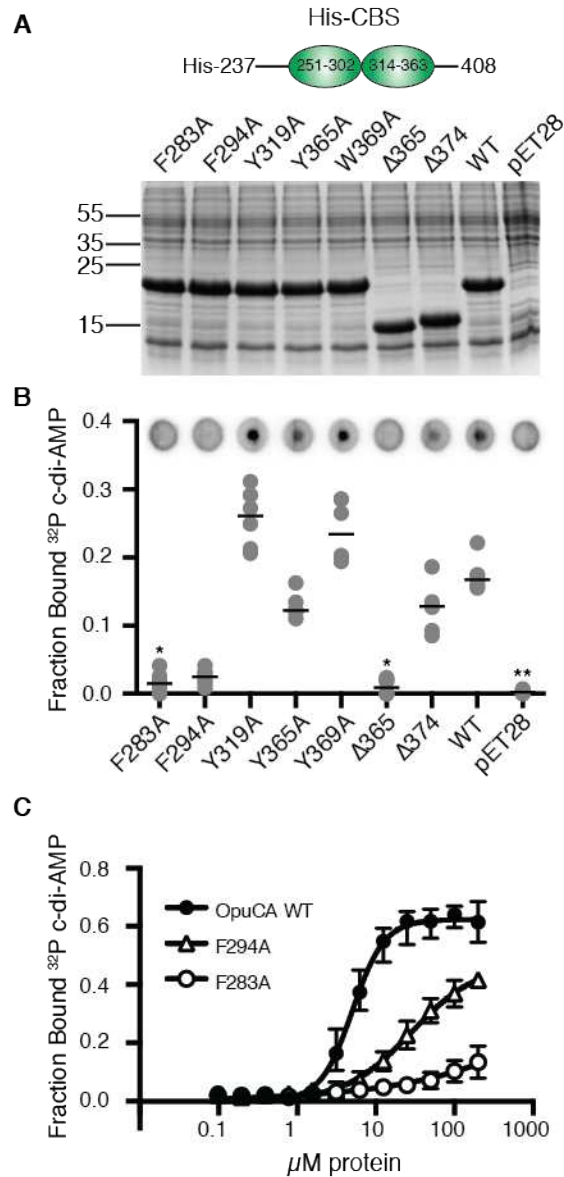


Fig. 5. Amino acids within the OpuCA CBS domain that are critical for c-di-AMP binding.

(A) Lysates from *E. coli* strains overproducing the His-CBS variants containing amino acid substitutions or C-terminal deletions, as well as lysates from the positive control His-CBS protein (WT) and the negative control (pET28b), separated on Coomassie stained polyacrylamide gel (n=6). (B) DRaCALAs with whole cell lysates shown in panel (A) and radiolabeled c-di-AMP. Representative spots are shown as well as the median fraction bound values and ranges (n=6). (C) Binding curve and K_d determination. Radiolabeled c-di-AMP and the purified His-CBS, His-CBS^{F283A} (F283A), and His-CBS^{F294A} (F294A) were used in DRaCALAs. Curves were fitted as in Fig. 1C and the K_d for c-di-AMP and the WT His-CBS protein determined. K_d values could not be determined for His-CBS^{F283A} and His-CBS^{F294A} because these variants showed reduced binding to c-di-AMP (WT: n=5, F283A & F294A: n=6, two independent protein purifications for each protein). Statistical analysis was done using a Kruskal-Wallis test, followed by Dunn's multiple comparison test. Adjusted p-values are indicated by asterisks (*), with * p < 0.05, ** p < 0.01.

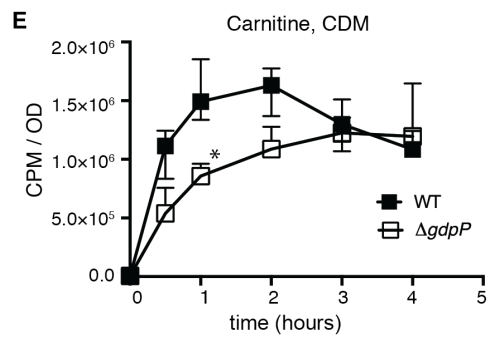
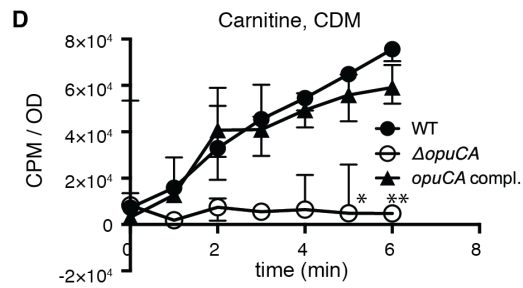
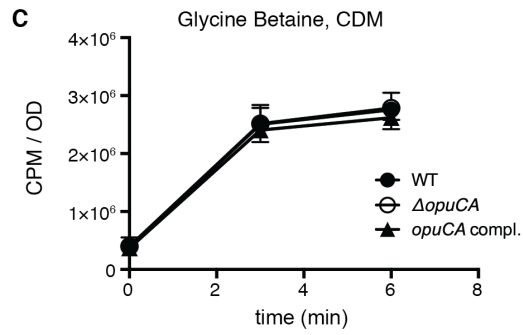
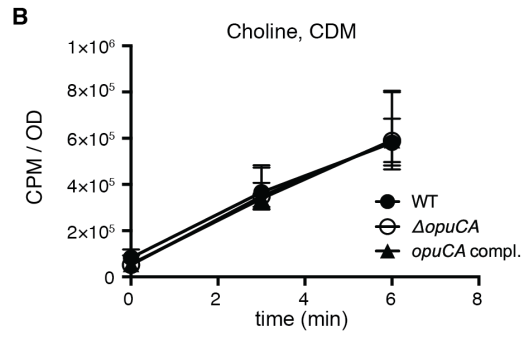
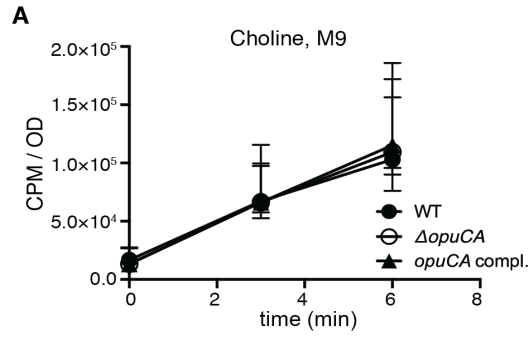


Fig. 6. The *S. aureus* OpuC transporter is a carnitine uptake system, and cellular c-di-AMP impacts carnitine uptake. Uptake of the compatible solutes in M9 (A) or CDM (chemically defined medium) (B-E). (A) Choline uptake in M9, (B) choline uptake in CDM (C) glycine betaine uptake in CDM, and (D) carnitine uptake in CDM was measured for the *S. aureus* strains LAC* pCL55 (WT), the *opuCA* mutant LAC* Δ *opuCA* pCL55 (Δ *opuCA*), and the complementation strain LAC* Δ *opuCA* pCL55-*opuCA* (*opuCA* compl.). Radiolabeled compatible solutes were added, aliquots were removed at the indicated time points, filtered, and the accumulated radioactivity measured. (E) Effect of c-di-AMP on carnitine uptake. Carnitine uptake was measured over a period of 4h for the strain LAC* (WT) and the high c-di-AMP strain LAC* Δ *gdpP* (Δ *gdpP*). Median values with ranges are plotted (n=3 for choline, all others n=4). Statistical analysis was performed using a Kruskal-Wallis test followed by Dunn's multiple comparison test (against WT at each time point). Adjusted p-values are indicated by asterisks (*), with * p < 0.05, ** p < 0.01.